Recent insights into inter-annual sandbar dynamics

Walstra, Dirkjan; Ruessink, BG

Publication date
2017

Document Version
Final published version

Published in
Proceedings of Coastal Dynamics 2017

Citation (APA)
Walstra, D., & Ruessink, BG. (2017). Recent insights into inter-annual sandbar dynamics. In T. Aagaard, R. Deigaard, & D. Fuhrman (Eds.), *Proceedings of Coastal Dynamics 2017: Helsingør, Denmark* (pp. 522-533). Article Paper No. 013

Coastal Dynamics 2017
Paper No. 013

RECENT INSIGHTS INTO INTER-ANNUAL SANDBAR DYNAMICS

Dirk-Jan Walstra[1,2] and Gerben Ruessink[3]

Abstract

Based on model hindcasts of the bar cycle at two locations along the Dutch coast, the dominant processes and mechanisms that govern the bar amplitude growth and decay during net inter-annual offshore migration, the occurrence of bar switches and the inter-site differences in the bar cycle return period (T_r) are identified. Bar growth and decay are closely related to the wave-induced longshore current as it affects the distribution of the cross-shore sediment transport. The modelling results suggest that cross-shore processes may trigger a bar switch in the case of specific antecedent morphological configurations combined with storm conditions. The deceleration of the offshore migration rate as the bar moves to deeper water (the morphodynamic feedback loop) contrasts with the initial enhanced offshore migration behavior of the bar for steeper slopes. The bed slope in the barred zone is the most important parameter governing T_r.

Key words: sediment transport, morphodynamics, process based modelling, sand bars

1. Introduction

Nearshore sandbars are present along most of the wave dominated sandy coasts wordwide. Sand bars are subaqueous features predominantly present across and just seaward of the surf zone (up to water depths of about 10 m). In general, up to 5 nearshore bars are found simultaneously in a cross-shore profile. They typically have a multi-annual lifetime, during which they most often behave in a cyclic, offshore directed manner with often a strong longshore coherence (Wijnberg and Terwindt, 1995; Shand et al., 1999, Kuriyama, 2002; Ruessink and Kroon, 1994). As the most seaward (outer) bar limits the amount of wave energy by enforcing waves to break, it controls the evolution of the shoreward located (inner) bars. Decay of the outer bar typically initiates a cascaded response in which the next (shoreward) bar experiences amplitude growth and net seaward migration. This in turn creates accommodation space for its shoreward neighbor and so on, eventually resulting in the generation of a new bar near the shoreline.

Although bars often show a strong longshore coherence over several km's, this does not imply that bars along the coast are all in the same phase of the bar migration cycle. Distinct shifts are observed in which for example the outer bar is attached to an inner bar. This is often referred to as bar switching (Wijnberg and Terwindt, 1995). It is defined as bars being alongshore discontinuous, either in a different phase of the bar cycle or with a completely different bar cycle return period (T_r, Plant et al., 1999; Wijnberg and Terwindt, 1995). For the latter case differences in T_r can be substantial (exceeding a factor 4) and appear to be continuously present in time (Wijnberg and Terwindt, 1995). This is here referred to as a persistent bar switch. Bar switches that separate sections with similar T_r are usually less persistent, as alongshore interactions cause bar switches to disappear when the adjacent bars are temporarily in a similar phase, here referred to as a non-persistent bar switch.

In this paper we provide a comprehensive overview of recent insights in inter-annual sandbar behavior. The following features that together encompass the main characteristics of the inter-annual bar morphology are discussed:

- The cross-shore transient bar amplitude response, that is, the transition from bar growth in the intertidal and across surf zone to bar decay at the seaward edge of the surf zone.
- The intra-site alongshore variability in cross-shore bar position, bar amplitude and the occurrence

[1]Deltares, Marine and Coastal Systems, PO Box 177, 2600 MH, Delft, The Netherlands. dirkjan.walstra@deltares.nl.
[2] Delft University of Technology, Faculty of Civil Engineering and Geosciences, Delft, The Netherlands.
[3]Utrecht University, Institute for Marine and Atmospheric Research, Department of Physical Geography, Utrecht, The Netherlands. b.g.ruessink@.uu.nl.

of non-persistent bar switches.

- The inter-site variability in the bar cycle return period which is typically accompanied by a persistent bar switch that separates two sections with different bar cycle return periods.

A comprehensive study approach is adopted in which observations of the nearshore morphology are combined with detailed forward model simulations in which the measured wave and water level conditions are used to force the model (referred to as brute forcing). Since the utilized model only considers cross-shore profile evolution, brute forcing does not cause unpractically long calculation times. A reference model was constructed, calibrated and validated. The reference model was applied to a single bar cycle return period at Noordwijk (The Netherlands) to calibrate the model's free parameters (see Walstra, 2016 for more details)

2. The cross-shore transient bar amplitude response

In this section we investigate bar amplitude growth and decay within one bar cycle. A detailed analysis, in which a hindcast at Noordwijk is combined with a range of schematic cases, is undertaken to determine the dependency of bar amplitude growth and decay on the offshore wave conditions (height, period and angle) and cross-shore bar location. Furthermore, the identified dominant processes that govern bar amplitude change are related to the observations to explain the transient bar amplitude change during the inter-annual net offshore bar migration (more details van be found in Walstra et al., 2012).

The temporal evolution of the profile in the hindcast simulation (Fig. 1, top) is characterized by relatively short (1 to 5 days) offshore migration periods, during wave events with offshore H_{rms} larger than about 2 m. Onshore migration was gradual and occurred during periods of moderately energetic, but just or non-breaking wave conditions (typically offshore H_{rms} < 1.5 m), which can last for several weeks to months at the study site. The temporal development of the bar amplitudes, A_b, (Fig. 1, bottom) clearly shows the decay of the two outer bars (bars 1 and 2). Notably, the amplitude of both outer bars responds only to major storm events. The inner bar amplitudes (bars 3 and 4) are more dynamic and show periods of bar growth not present for the two outer bars. All bars generally have a comparable migration response, dX_b/dt, but the associated amplitude change, dA_b/dt, is less consistent as individual bars may grow and decay simultaneously. For example, at t=550days, the largest profile response event with the largest simultaneous offshore bar migration, bar 2 decayed whereas bars 3 and 4 became more pronounced. In accordance with Ruggiero et al. (2009), dA_b/dt is sensitive to the water depth above the bar crest, h_{Xb}.

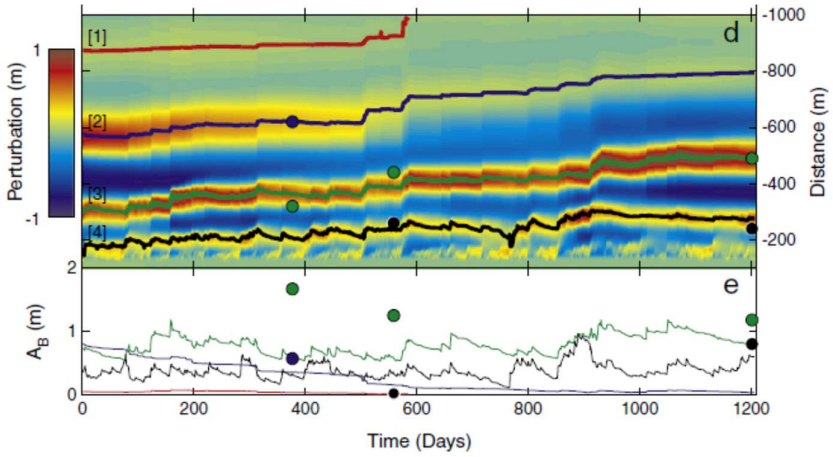

Figure 1. Time series of (top) time stack of predicted profile perturbation and indication of bar crests ([1], [2], [3], [4], line colors indicate bar crest position), and (bottom) predicted bar amplitudes A_b, (circles indicate the measured crest positions (top) or bar amplitudes (bottom). t=0 days corresponds to 19 June 1984 00:00 hh:mm.

As a first step to determine when bars grow and decay, dA_b/dt, extracted from Fig. 1, was correlated with wave parameters. The offshore wave height and the wave height at the bar crest result in similar

correlations. Interestingly, the sign of the correlation changes from bar 1 toward bar 4. This indicates the opposite response to similar wave conditions, also observed in Fig. 1. The correlation for the absolute wave angle is generally smaller than for the wave height, but is always positive. A high correlation for the local longshore surface shear stress component due to wave breaking, $\tau_{sw,y}$, for the two outer most bars (3 and 4) was found. This indicates that longshore forcing may play a significant role in the bar growth.

In order to separate the interaction between the forcing parameters and the bar morphology a range of wave conditions and water level combinations (H_{rms}, T_p, θ, η) was considered for the t=0 profile. The initial bar amplitude response very clearly revealed that the incident wave angle has a major impact on the bar amplitude response. For normally incident waves bar decay dominated whereas for increasing wave angles bar growth was predicted.

The question now arises as to why the angle of wave incidence is so important to bar growth and decay. Conceptually, obliquely incident waves induce longshore wave-driven currents which will influence the magnitude of bed shear stresses and subsequently the cross-shore distribution of the sediment transport via enhanced sediment stirring. This is illustrated in Figs. 2a–f by comparing the distribution of relevant model outputs across bar 3 for two conditions with identical water level, offshore wave height and period (H_{rms}=1.7 m, T_p=8 s, η=0 m), but different wave angles (θ = 0° versus θ = 60°). The two conditions induce an opposite dA_b/dt response during offshore bar migration. Fig. 2f shows the initial and final perturbations from which it is clear that the oblique waves induce a growth of bar 3, whereas for the shore-normal waves the bar decays. The observed morphological response is clearly linked to the distribution of the total cross-shore transports, $S_{x,tot}$ (Fig. 2e). The shore-normal wave condition results in a maximum offshore $S_{x,tot}$, $S_{x,max}$, just seaward of the bar crest while for the oblique wave condition $S_{x,max}$ is located about 20 m landward of the bar crest. From Figs. 2g–l it is clear a similar effect is present for onshore bar migration. This difference is caused by the different forcing mechanisms that drive the cross-shore and longshore currents. The local distribution of the cross-shore currents over the bar is particularly sensitive to variations in the local water depth as the cross-shore variation in wave height is limited. This causes the location of the maximum cross-shore currents to coincide with the bar crest location. As the wave-driven longshore current originates from $\tau_{sw,y}$, it has a very similar distribution resulting in a concomitant landward shift of the longshore current. Furthermore the longshore current is typically much larger than the cross-shore current for oblique waves. Since the sediment concentration is based on the current magnitude to approximately the 4th power, its cross-shore distribution is mainly influenced by the longshore current (Fig. 2d). So in case of oblique incident waves, longshore currents will have a considerable influence on the distribution of the cross-shore sediment transports. If the offshore transport peak is shifted landward of the bar crest, bar amplitude growth instead of decay is predicted during offshore bar migration (and vice versa, see Figs. 2g-l). The strong dependency on the longshore current explains the observed transient bar amplitude response during the net inter-annual offshore migration. For bars in relatively shallow water wave breaking is more frequent, promoting net bar amplitude growth in case of oblique wave incidence, whereas in deeper water wave breaking on the bars is limited, leading to net bar amplitude decay.

3. The occurrence of non-persistent bar switches (intra-site variability in bar characteristics)

Bar switching is typically an indication of a distinct phase shift in the bar cycle (Wijnberg and Terwindt, 1995; Shand, 2003) where an outer bar is attached to an inner bar or where bars are detached completely, resulting in a fork-like configuration. Although bars can switch under natural conditions, shoreface nourishments may also trigger switches. For example at Noordwijk, The Netherlands, the net offshore bar migration was delayed immediately landward of a shoreface nourishment, while elsewhere net offshore bar migration continued. This spatially discontinuous offshore migration resulted in bar switches that lasted about one year (Ojeda et al., 2008). Although natural and nourishment-induced bar switching events are largely similar, little is known about the physical processes that govern this type of morphological response under natural conditions.

In this section it is investigated 1) to what extent cross-shore processes can initiate, amplify or dampen alongshore sandbar variability on km-scale and 2) to identify the relative importance of wave forcing and antecedent morphology on the predicted large scale alongshore variability. To that end, the profile model is applied on 24 transects with an alongshore spacing of 250 m at a 6 km coastal section near Noordwijk.

During the considered period, continuous alongshore bars are followed by natural bar switching events which in time transform back to continuous alongshore bars. To identify the importance of cross-shore processes, model predictions initialized with a relatively alongshore uniform set of profiles are compared with predictions starting in a year when a bar switch was present.

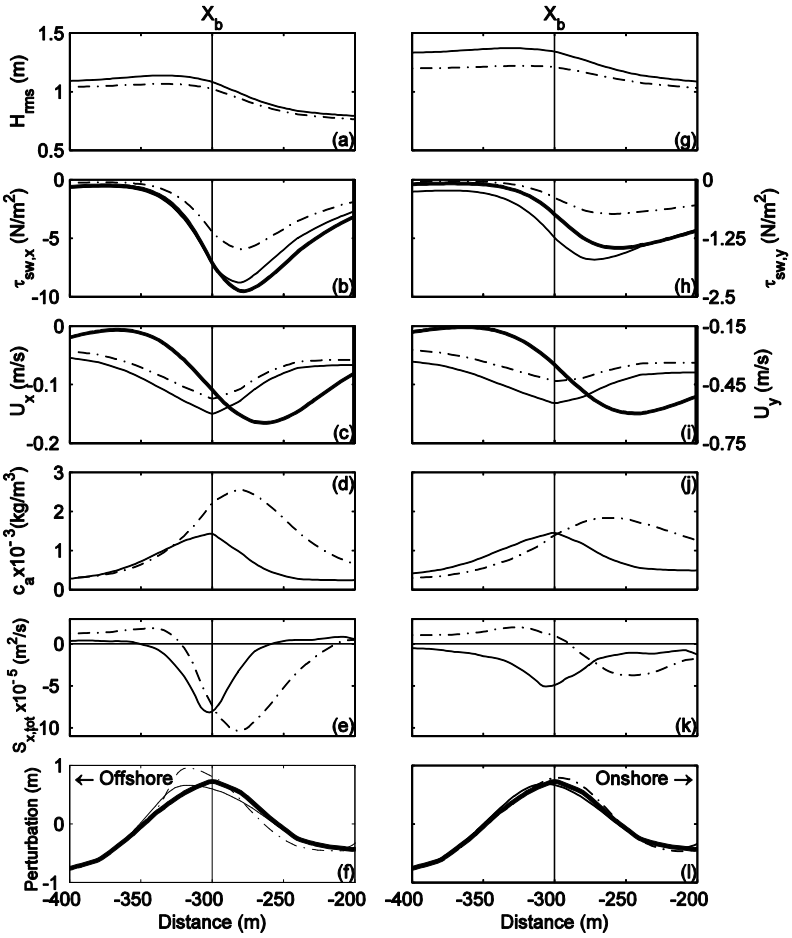

Figure 2. Comparison predictions with oblique (θ = 60°, dash-dotted lines) and shore normal (θ = 0°, solid lines) incident wave angles for η = 0 m (a–f) and η = 1 m (g–l) for H_{rms} = 1.7 m and T_p = 8 s (vertical lines indicate bar crest). Cross-shore distribution of: (a, g) wave height, (b, h) cross-shore wave forcing and longshore wave forcing (thick line), (c, i) cross-shore velocities and longshore velocities (thick line), (d, j) near-bed reference concentration, (e, k) cross-shore sediment transport, and (f, l) initial profile (thick solid line) and predicted profiles after 1 day.

The considered period (1987-1992) was selected as it included the initiation of a bar switch (1988) that had vanished two years later (Fig. 3). Since the bar switch is not present in the 1987 bar morphology, it can be investigated whether the cross-shore processes can initiate a bar switch from relatively alongshore uniform bars. The opposite (i.e. can the model predict the end of a bar switch when it is present in the initial bar morphology) is tested with the simulations starting in 1989. The basis of the analysis is a comparison of the observed and predicted profile perturbations. Although the simulations at each transect were independent, we combined the predicted profile development into a top view of the perturbations of the 6 km study area for two sets of simulations starting from the 1987 (Fig. 3) and 1989 profiles (Fig. 4).

The initial (1987) and predicted morphological development from 1988 to 1990 are compared with the observations in Fig. 3. The offshore migration and amplitude growth of the inner bar coincided reasonably well after 1 year (year 1988, compare Figs. 3b and e). However, the offshore migration of the outer bar was significantly over-estimated. Besides the over-estimated offshore migration of both bars in the following

years, X_b (and also h_{Xb}) remained alongshore coherent, in contrast to the observations. In the southern section the outer bar is interpreted as being no longer present as it has decayed considerably, resulting in a relict feature without alongshore coherence. From 1989 to 1990, the former inner bar (which by now had become the outer bar) was predicted to gradually migrate further offshore. The predicted alongshore variability remained approximately constant. As the bar switch had disappeared by 1990 (Fig. 3d), the final prediction (Fig. 3g) resembled the observations (Fig. 3d) fairly well. However, the model completely failed to predict the observed initiation and decay of the bar switch.

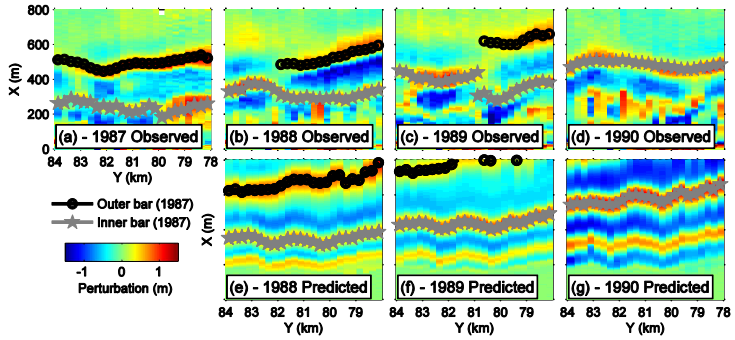

Figure 3. Observed (top row) and predicted (bottom row) profile perturbations from 1987 to 1990, black (grey) line tracks the outer (inner) bar starting from 1987.

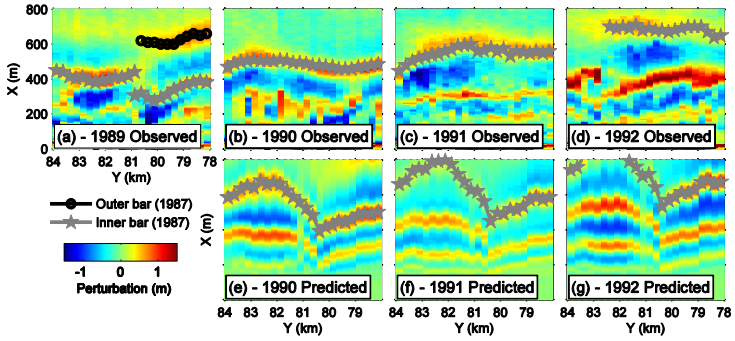

Figure 4. Observed (top row) and predicted (bottom row) profile perturbations from 1989 to 1992, black (grey) line tracks the outer (inner) bar starting from 1987.

Interestingly, similar to the observations, the initial 1989 inner bar switch was almost removed in the predictions (compare Figs. 4b and e). The transformation of the concave shape of the inner bar at y=81 to 84 km in 1989 to a convex shape in 1990 qualitatively agrees with the observations. In the model this change in plan shape was caused by the alongshore variability in the water depth above the 1989 bar crest, $h_{x,b}$. At the center of the convex shape (y=82.25 km) the bar was most pronounced (i.e. small $h_{x,b}$) whereas at the distal ends $h_{x,b}$ was initially larger and therefore limited the offshore migration from 1989 to 1990. The alongshore variability of the inner bar was, however, significantly over-estimated. The alongshore variability was predicted to increase with time as the southern section of the bar migrated further offshore and decayed more than the northern section. The enhanced offshore migration in the southern section created accommodation space for a new inner bar, which in 1991 nearly attached to the outer bar at y=80.5km (Fig. 4f). However, probably due to the absence of alongshore interaction, this connection did not occur during the following year. By 1992 a new bar switch was present in the observations which showed some similarities with the final predicted morphology.

A common finding from both simulation periods is that the model largely maintains the initial alongshore variability throughout the simulations. As a consequence the model fails to predict the observed generation and decay of bar switches. In additional simulations the comparison with the observed

alongshore variability clearly shows that the simulations initialized with profiles that contained bar switches (years of initialization: 1988, 1989 and 1992) persistently over-estimated the alongshore variability. In contrast, periods that were initially relative alongshore uniform, but during which a bar switch developed within the 3-year simulation period, the alongshore variability was under-estimated (e.g. years of initialization: 1987 and 1991). For periods where the observed alongshore uniformity was approximately constant, there was mostly good agreement in (e.g. years of initialization: 1990, 1993 and 1994).

Furthermore, additional simulations were carried out in which the initial profiles were subjected to wave forcing time series with higher and lower energy. Despite the clear effect of the wave forcing on the alongshore averaged bar morphology, the alongshore variability of the bar crest positions appeared to be relatively unaffected for alongshore uniform initial profiles. In case a bar switch is present in the initial profiles, the alongshore variability was comparable for the bar sections on either side of the bar switch. However, the alongshore averaged bar morphology at each side of the bar switch responded differently to the modified wave forcing. This is further investigated in Fig. 5, where the offshore bar migration at both sides of the bar switch had a dissimilar response to the modified wave forcing. The southern area experienced an accelerated offshore migration relative to the northern area in case of the more energetic wave forcing (WF1987 and WF1989), whereas such a response was absent for the less energetic wave forcing (WF1995), see Fig. 5.

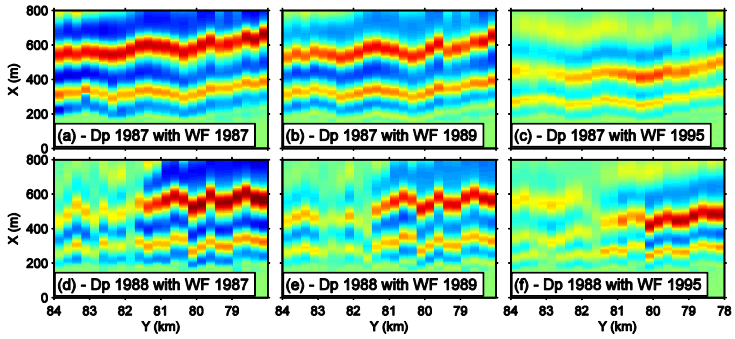

Figure 5. Perturbations of the final predicted morphological development for different combinations of profile initialization and wave forcing time series. Starting from the 1987 (top row) and 1988 (bottom row) profiles imposed with 1987-1990 (WF1987, left column), 1989-1992 (WF1989, middle column) and 1995-1998 (WF1995, right column) wave time series.

Because our model is reasonably accurate in the absence of bar switches, we infer that the increased model-error in the presence of bar switches (Figs. 3 and 4) is primarily caused by three-dimensional processes, such as flow patterns induced by the alongshore variable morphology which are not accounted for by the model. It is fair to say, however, cross-shore processes also influenced the alongshore variability even to the extent that bar switches were nearly removed when bars at either side of the switch were temporary in a similar phase (Figs. 5d-f). The water depth above the bar crest, h_{Xb}, was found to be of primary importance as, for a given wave forcing, it largely controlled the bar amplitude and bar migration response. For example, the alongshore variations in h_{Xb} in the 1989 profiles resulted in a non-linear morphological response that considerably increased the alongshore variability of the southern section (y>81 km, see Fig. 4).

The increased phase differences at either side of the bar switch in the 1988 bathymetry predicted by the WF1987 and WF1989 scenarios were both induced during periods with increased wave action (Fig. 6). However, during later periods with similar wave forcing such a response was absent. These outcomes show that a specific state of the morphology subjected to a period with energetic wave forcing can result in an alongshore varying response also when only cross-shore processes are considered. Furthermore, taking into consideration that 3D effects (such as rip currents) could further enhance the alongshore variability, we suspect that the generation of bar switches, similar to the findings of Shand et al. (2001), is the outcome of a particular morphological state and wave forcing combination (see also Walstra et al. 2015).

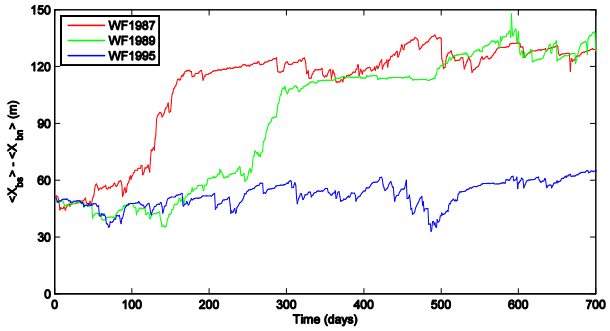

Figure 6. Temporal development of the difference between the alongshore averaged bar position south, $<X_{bs}>$, and north, $<X_{bn}>$, of the bar switch at y=81.50 km for the 1987-1991, 1989-1992 and 1995-1998 wave forcing time series starting from the 1988 profiles.

4. Variability in the inter-annual nearshore sandbar cycle period between sites

4.1. *Environmental settings*

We utilize the profile model to identify the dominant environmental variables and the associated mechanisms that govern inter-site differences in T_r. To that end, the model is applied at the locations Noordwijk and Egmond 42 km apart. The sites are located just South and North of the IJmuiden harbor moles with distinctly different bar cycle return periods. The model is utilized to investigate the influence of various environmental parameters on T_r. A range of model simulations are evaluated by comparing the predicted bar cycle return periods for various combinations of environmental variables from the Noordwijk and Egmond sites. The considered variables comprise the wave forcing (viz. wave height and incident wave angle), sediment size, and various geometric profile properties (viz. bar size, bar location and profile steepness). Subsequently, the underlying processes that predominantly govern T_r are identified.

Due to the concave shape of the Holland Coast, the coastline orientation at Egmond (277 °N) and Noordwijk (298 °N) differs by about 21°. The sediment at Egmond is markedly coarser than at Noordwijk (D_{50} is 265 µm compared to 180 µm at Noordwijk). The time-averaged profiles derived for Noordwijk and Egmond based on the annual profile surveys (Wijnberg and Terwindt, 1995) for the period 1965 to 1998 clearly reveal distinct differences in profile slopes between both sites (Fig. 7).

Both at Egmond and Noordwijk mostly three bars are present (Wijnberg and Terwindt, 1995; Pape et al, 2010). The time stack plots (Figs. 8a,b) clearly reveal the inter-annual cyclic bar characteristics. That is, bar initiation in the inter-tidal region ($x \approx 200$ m), gradual offshore migration and amplitude growth and finally gradual decay at the seaward limits of the surf zone. However, the difference in bar cycle return period between both sites is striking. Estimates of T_r, derived earlier with a complex EOF method are 3.9 and 15.1 years for Noordwijk and Egmond, respectively (Ruessink et al., 2003). Furthermore, the bars at Egmond are noticeably wider and higher. We considered the period from 1 January 1990 to 31 December 1999 for which detailed hourly and 3-hourly wave observations (root-mean-square wave height H_{rms}, peak wave period T_p and wave direction θ) were available for Noordwijk and IJmuiden (about 17 km south of Egmond, respectively. Apart from the waves from the southwestern direction, the wave height at Egmond is larger. Especially for the northwestern direction this difference increases as Egmond is more exposed to the North Sea. Differences in the time-mean wave period are relatively small.

4.2. *Approach*

The main objective is to identify which environmental parameters and processes primarily govern the bar cycle duration. To that end we apply the calibrated Noordwijk model (Walstra et al., 2012) to a profile at Egmond as well. Although profile models typically require a site-specific calibration (e.g. Ruessink et al., 2007), we maintain the Noordwijk model settings in the application at the Egmond site. Only the site specific environmental variables from Egmond are used (i.e., profile, d_{50} and time series of the waves and waterlevels). It is not our aim to achieve an optimal performance at Egmond (i.e. best agreement with the

observed inter-annual profile evolution) as long as the model is able to predict a significant difference in T_r between both sites. That will allow us to generate consistent predictions for both sites in which, for example, one specific (known) variable is modified. This approach allows us to identify the influence of the main environmental parameters such as wave height, near shore profile shape and sediment size on T_r (Walstra et al., 2016). As a first step, the predictions for both sites are evaluated. Next, the main environmental variables will be interchanged to identify the relative contribution of the wave climates, profiles and sediment size to changes in the bar cycle return period (i.e. the Egmond wave climate is combined with the Noordwijk profile and vice versa). To identify the mechanisms and processes that govern T_r detailed schematic simulations are conducted and analyzed in which, for example, the influence of the profile slope on T_r is quantified. The bar cycle return period T_r was determined by the time it takes a bar to be at the same cross-shore position as its predecessor. Ruessink et al. (2003) showed that the complex EOF analysis is a robust method to derive T_r and it is therefore also used in this study.

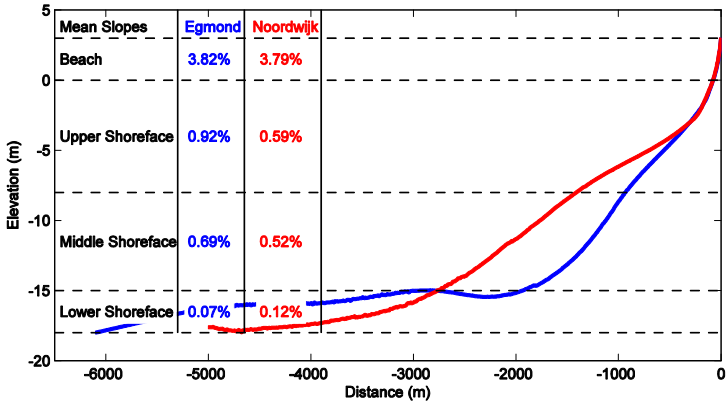

Figure 7. Time-averaged profiles for Noordwijk and Egmond on the same cross-shore axis with the origin for both at NAP 0 m.

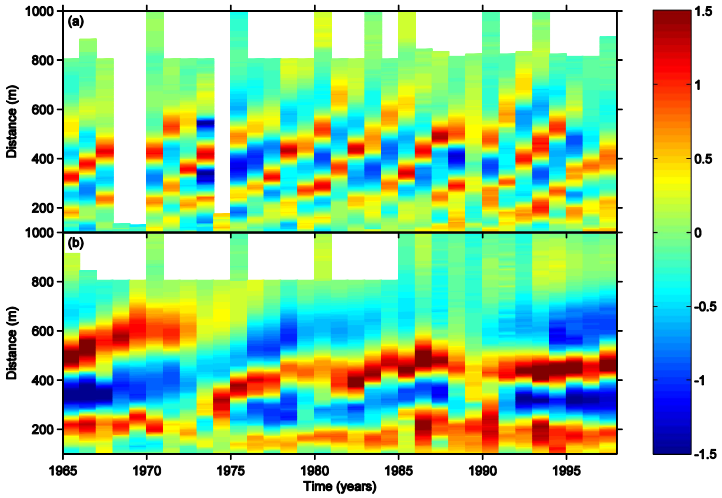

Figure 8. Profile perturbations of the time averaged near-shore profile are shown for a) Noordwijk and b) Egmond.

4.3. *Results*

From the comparison of the predicted profile development (Fig. 9) the difference in bar cycle duration stands out immediately. The bar cycle period for Noordwijk is 4.8 years (Scenario NN, see Table 1) which compares well to that derived from the observations for the same period (T_r = 3.9 years). For Egmond (Scenario EE) the predicted T_r of 8.7 years is significantly larger. However, it is still a significant under-

estimation of the value derived from the profile surveys (T_r = 15.1 years). Since we are primarily interested in identifying the causes for the difference in the bar cycle period, we consider the model performance at Egmond to be adequate since the model predicts a significant difference in T_r between both sites.

The initial profile and wave climate have a profound impact on the resulting profile evolution. Imposing the slightly more energetic Egmond wave climate on the Noordwijk profile (Scenario NE) results in a 50% reduction of the bar cycle period. The opposite occurs when subjecting the Egmond profile to the Noordwijk wave climate (Scenario EN, see Fig. 10b): the bar cycle period is almost doubled to 14.6 years. Although the Egmond wave climate reduced T_r, the wave climate increases the bar zone width by about 200 m and also results in slightly increased maximum bar amplitude. Due to the increased T_r, the bar zone width is difficult to determine for Scenario EN, but the results seem to suggest that it decreases by at least 100 m. Furthermore, the maximum bar amplitude in this scenario is about 0.5 m less compared to the Egmond reference case (Scenario EE, see Fig. 9b). Consistent with Ruessink et al. (2003), the energy level of the wave climate appears to influence T_r significantly. However, the effect of the initial profile and bar morphology has an even larger influence. Comparing T_r for the four scenarios (summarized in Table 1) an indication of the relative importance of the initial profiles and wave climates can be obtained. The interchange of wave climates results in a change of T_r of about 200% (compare scenarios NN & NE and EE & EN). The influence of the initial profile, bar morphology and sediment size results in a variation T_r of about 300%. For example, the Egmond climate on the Noordwijk profile results in a T_r of 2.4 years compared to T_r = 8.7 years for the Egmond profile.

The effect of the profile slope was further investigated by considering morphostatic simulations (i.e. no bed updating) starting from schematic profiles in which identical bars (with the crest at identical water depth) are combined with bed slopes representative for Egmond and Noordwijk which were subjected to the full 9.5 year Noordwijk wave and water level time series. Detailed comparisons of wave height, undertow and sediment transport at the crest of the bars clearly confirmed that, despite the identical wave height at the top of the bar (Fig. 11a), the undertow (depth-averaged return flow) is indeed larger due to more intense wave breaking at the bar crest for the steeper Egmond profile (Fig. 11b). The enhanced turbulence levels due to the wave breaking and the increased return flow velocities consequently enhance the offshore sediment transports (Fig. 11c). Potentially, this would induce an enhanced offshore bar migration and thus a reduction in T_r.

In the hindcast simulations at Egmond this initial response apparently does not result in an increased T_r. Therefore, it is assumed that the cumulative effect of the morphodynamic feedback between the barred profile and the wave forcing primarily governs T_r. To estimate T_r we conduct a set of 1-day simulations starting from plane profiles in which a bar is placed at 21 equidistant locations across the bar zone. In order to exclude the effect of the transient bar amplitude response (i.e. the change from growth to decay as the bar migrates across the surf zone) we considered a bar with a constant shape. For each simulation the daily migration rate and bar amplitude response are determined by considering the change in the horizontal and vertical bar crest position. Subsequently, the daily migration rates are integrated over the set of 21 simulations to estimate the time it takes for a bar to migrate across the bar zone as a proxy for T_r.

The importance of the bed slope implies that h_{Xb} and the morphodynamic feedback loop primarily govern T_r. Despite more intense wave breaking and an initial enhanced offshore migration rate, the overall effect of a steeper profile is an increased T_r as it causes:

1) A relatively larger increase in h_{Xb} as a bar gradually migrates offshore which in turn causes fewer waves to break on the bar and consequently reduces the offshore bar migration.
2) Enhanced wave breaking results in relatively larger bars (e.g. see Fig. 10b) that will also reduce the offshore migration. Although a larger bar amplitude implies a somewhat smaller h_{Xb} at the same cross-shore location (and T_r), the increase in h_{Xb} as a bar migrates offshore dominates the T_r response.
3) An increased water depth where bar decay sets in due to more intense wave breaking. Combined with the more energetic wave climate this increases the bar zone width at Egmond by about 200 m compared to Noordwijk (as was both observed –Figure 8 - and predicted – Figure 10). Therefore it takes longer for the bars to migrate across this region (e.g. a mean offshore migration rate of 40 m/year would lead to a five year increase in T_r).

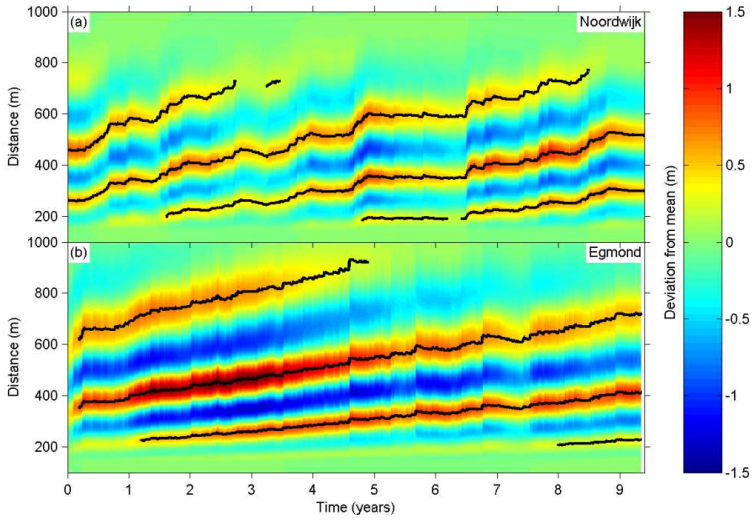

Figure 9. Predicted profile perturbations for a) Noordwijk (Scenario NN) and b) Egmond (Scenario EE).

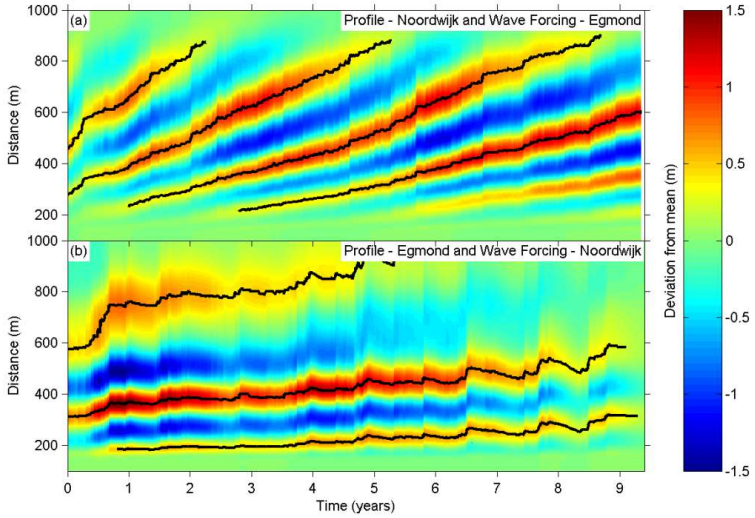

Figure 10. Predicted profile perturbations for scenarios with swapped wave forcing: a) Noordwijk profile with wave forcing from Egmond (Scenario NE) and b) vice versa (Scenario EN).

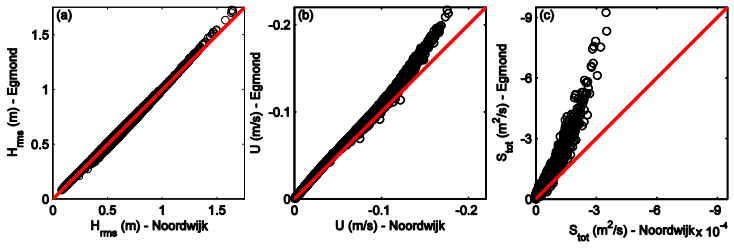

Figure 11. Comparison of the root-mean-square wave height H_{rms} (a), depth-averaged return flow U (b) and total sediment transport S_{tot} (c) at the top of an identical bar crest combined with the middle and lower shoreface profiles of Noordwijk and Egmond. Red line indicates equality between Egmond and Noordwijk.

Table 1. Simulations for Noordwijk and Egmond with interchanged wave forcing, profiles and sediment diameter.

Scenario	Profile & Sediment	Wave Time Series	Cycle Period (T_r, years)
NN	Noordwijk	Noordwijk	4.8
EN	Egmond	Noordwijk	14.6
NE	Noordwijk	Egmond	2.4
EE	Egmond	Egmond	8.7

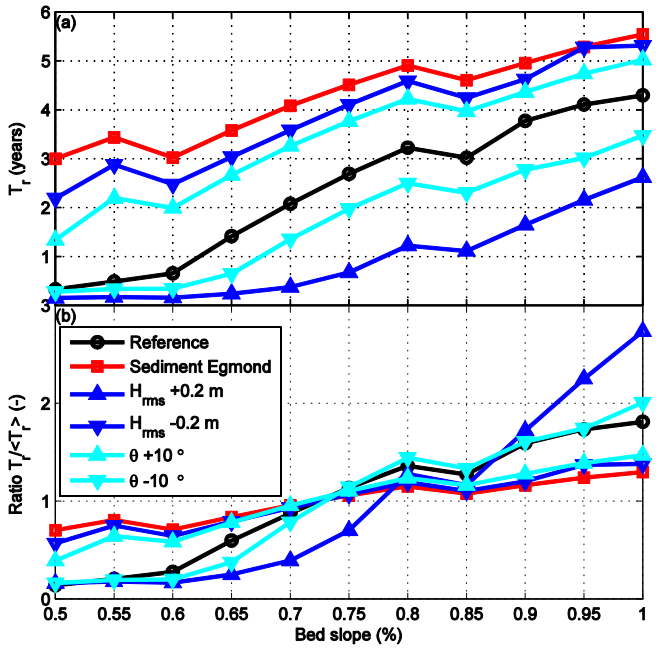

Figure 11. Absolute T_r (a) and the change in T_r relative to the T_r averaged over all considered bed slopes $T_r/\langle T_r \rangle$ (b) as a function of the bed slope. The reference case is based on the Noordwijk environmental parameters.

5. Conclusions

Bars experience amplitude growth in the inner and middle surf zone regions due to enhanced sediment stirring on the landward bar slope and trough by the breaking-induced longshore currents. The increased sediment concentration in these regions can shift the peak of the cross-shore transport landward of the bar crest. This shift induces bar amplitude growth during offshore migration. During onshore bar migration the enhanced sediment stirring by the longshore current results in increased transport from the landward trough toward the bar crest, promoting bar amplitude growth. The water depth at the bar crest, h_{Xb}, and the angle of wave incidence, θ, control the generation of the longshore current. For bars in shallow water the bar amplitude response and θ are strongly related, due to the relatively strong longshore current that waves breaking under an angle generate. This highlights the hitherto largely ignored importance of the wave angle on cross-shore bar dynamics.

Bar decay at the seaward boundary of the surf zone is the result from a reduction of the number of breaking waves decreases the relevance of the associated longshore currents at bars in deeper water. This causes the undertow to dominate the cross-shore sediment transports. Consequently the transport peaks will coincide with the bar crest location which results in net bar amplitude decay at larger water depths.

Cross-shore processes are not able to dissipate a bar switch, as in contrast to the observed bar behavior, predicted bar morphologies on either side of the switch remain in a different phase. The alongshore variability is only temporarily reduced when the bars on either side are occasionally located in a similar cross-shore position.

Only under specific bar configurations and high wave-energy levels an increase in alongshore variability is predicted. This suggests that cross-shore processes may trigger a switch in the case of specific antecedent morphological configurations combined with storm conditions.

The model simulations illustrate that T_r is found to be positively correlated with sediment diameter and bar size, while T_r is negatively correlated with the wave forcing and profile slope. The simulations starting from composite profiles in which bar size, profile slope and sediment size were varied, clearly identified the bed slope in the barred zone to be the most important parameter that governs T_r. The application of the Egmond instead of the Noordwijk wave climate reduces T_r by a factor 3 to 4. However, the predicted T_r at Egmond is about twice as large, which is primarily originating from the difference in the upper profile slope and the larger sediment diameter at Egmond.

The sensitivity of T_r to the upper profile slope arises from the importance of the water depth above the bar crest (h_{Xb}) for sandbar response. As a bar migrates seaward, a steeper slope results in a relatively larger increase in h_{Xb}, which reduces wave breaking and subsequently causes a reduced offshore migration rate (and hence an increase in T_r). Therefore, we conclude that the morphodynamic feedback loop is significantly more important than the initially larger offshore bar migration due to the more intense wave breaking in case of a steeper profile slope.

References

Kuriyama, Y., 2002. Medium-term bar behavior and associated sediment transport at Hasaki, Japan. *Journal of Geophysical Research* 107 (C9), 3132. doi:10.1029/2001JC000899.

Ojeda, E., Ruessink, B.G., Guillen, J., 2008. Morphodynamic response of a two-barred beach to a shoreface nourishment. *Coastal Engineering* 55(12), 1185–1196. doi:10.1016/j.coastaleng.2008.05.006

Pape, L., Kuriyama, Y. & Ruessink, B.G., 2010. Models and scales for nearshore sandbar behavior. *Journal of Geophysical Research-Earth Surface*, 115 (F03043).

Plant, N.G., Holman, R.A., Freilich, M.H., Birkemeier, W.A., 1999. A simple model for inter-annual sandbar behavior, *Journal of Geophysical Research – Oceans* 104-C7, pp 15,755–15,776.

Ruessink, B.G., Kroon, A., 1994. The behaviour of a multiple bar system in the nearshore zone of Terschelling: 1965–1993. Marine Geology 121, 187–197. doi:10.1016/0025-3227(94)90030-2.

Ruessink, B.G., Miles, J.R., Feddersen, F., Guza, R.T., Elgar, S., 2001. Modeling the alongshore current on barred beaches. *Journal of Geophysical Research* 106, 22451–22463. doi:10.1029/2002JC001505.

Ruessink, B.G., Wijnberg, K.M., Holman, R.A., Kuriyama, Y., van Enckevort, I.M.J., 2003a. Intersite comparison of inter-annual nearshore bar behavior. *Journal of Geophysical Research* 108 (C8), 3249. doi:10.1029/2002JC001505.

Ruessink, B.G., Kuriyama, Y., Reniers, A.J.H.M., Roelvink, J.A., Walstra, D.J.R., 2007. Modeling cross-shore sandbar behavior on the timescale of weeks. *Journal of Geophysical Research-Earth Surface* 112 (F3), 1–15. doi:10.1029/2006JF000730.

Shand, R.D., Bailey, D.G., Shephard, M.J., 1999. An inter-site comparison of net offshore bar migration characteristics and environmental conditions. *Journal of Coastal Research* 15, 750–765.

Shand, R.D., 2003. Relationships between episodes of bar switching, cross-shore bar migration and outer bar degeneration at Wanganui, New Zealand. Journal of Coastal Research 19 (1), 157-170, ISSN 0749-0208.

Walstra, D.J.R., Reniers, A.J.HM., Ranasinghe, R., Roelvink, J.A., Ruessink, B.G., 2012. On bar growth and decay during inter-annual net offshore migration. *Coastal Engineering* 60, 190–200. doi:10.1016/j.coastaleng.2011.10.002.

Walstra, D.J.R., Ruessink, B.G., Reniers, A.J.H.M. and Ranasinghe, R., 2015. Process-based modeling of kilometer-scale alongshore sandbar variability. *Earth Surface Processes and Landforms*, 40, 995–1005. doi: 10.1002/esp.3676.

Walstra, D.J.R., Wesselman, D.A., van der Deijl, E.C., Ruessink, B.G., 2016. On the intersite variability in inter-annual nearshore sandbar cycles. *Journal of Marine Science and Engineering*, 4(1), 15. doi:10.3390/jmse4010015.

Walstra, D.J.R., 2016. On the anatomy of nearshore sandbars: a systematic exposition of inter-annual sandbar dynamics. Phd-thesis, Delft University of Technology. ISBN 978-94-6168-647-9, doi:10.4233/uuid:3f86bf04-c6af-486f-b972-bd228d84ebed.

Wijnberg, K.M., Terwindt, J.H.J., 1995. Extracting decadal morphological behavior from high-resolution, long-term bathymetric surveys along the Holland coast using eigenfunction analysis. *Marine Geology* 126 (1–4), 301–330.